Article

Glassy and Polymer Dynamics of Elastomers by ¹H Field-Cycling NMR Relaxometry: Effects of Cross-Linking

Francesca Martini, Elisa Carignani, Francesca Nardelli, Elena Rossi, Silvia Borsacchi, Mattia Cettolin, Antonio Susanna, Marco Geppi,* and Lucia Calucci*
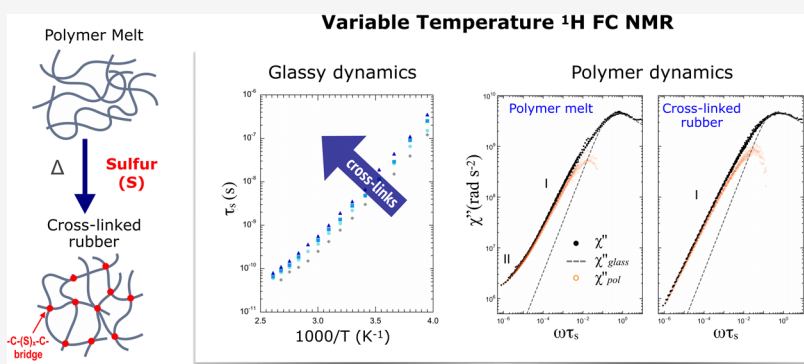
Read Online

ACCESS | Metrics & More | Article Recommendations | Supporting Information

ABSTRACT: ¹H spin lattice relaxation rate (R_1) dispersions were acquired by field-cycling (FC) NMR relaxometry between 0.01 and 35 MHz over a wide temperature range on polyisoprene (IR), polybutadiene (BR), and poly(styrene-*co*-butadiene) (SBR) rubbers, obtained by vulcanization under different conditions, and on the corresponding uncured elastomers. By exploiting the frequency−temperature superposition principle, $\chi''(\omega\tau_s)$ master curves were constructed by shifting the total FC NMR susceptibility, $\chi''(\omega) = \omega R_1(\omega)$, curves along the frequency axis by the correlation times for glassy dynamics, τ_s. Longer τ_s values and, correspondingly, higher glass transition temperatures were determined for the sulfur-cured elastomers with respect to the uncured ones, which increased by increasing the cross-link density, whereas no significant changes were found for fragility. The contribution of polymer dynamics, $\chi''_{pol}(\omega)$, to $\chi''(\omega)$ was singled out by subtracting the contribution of glassy dynamics, $\chi''_{glass}(\omega)$, well represented using a Cole−Davidson spectral density. For all elastomers, $\chi''_{pol}(\omega)$ was found to represent a small fraction, on the order of 0.05− 0.14, of the total $\chi''(\omega)$, which did not show a significant dependence on cross-link density. In the investigated temperature and frequency ranges, polymer dynamics was found to encompass regimes I (Rouse dynamics) and II (constrained Rouse dynamics) of the tube reptation model for the uncured elastomers and only regime I for the vulcanized ones. This is clear evidence that chemical cross-links impose constraints on chain dynamics on a larger space and time scale than free Rouse modes.

INTRODUCTION

Linear polymer melts show dynamics over a wide frequency scale, from the fast scale of local segmental dynamics and internal motions to the very slow scale of diffusive motions of the center of mass of the polymer chains. Segmental motions within the so-called Kuhn segment with characteristic time τ_s are responsible for "glassy dynamics" connected with the structural relaxation or α-process ($\tau_s = \tau_\alpha$). If mobile side groups exist in the polymer, the main-chain local segmental motions may be supplemented and superimposed to reorientations of such groups. The connection of segments into chains results in slower polymer-specific collective dynamics, indicated in the following as "polymer dynamics". For polymers with molar mass M below the critical value M_e (average molar mass between entanglements), Rouse theory[1] well describes polymer dynamics. Longer chains ($M > M_e$)

form physical entanglements, and their dynamics has been described by the tube reptation (TR) model developed by De Gennes[2] and Doi and Edwards,[3] by the *n*-renormalized Rouse model,[4−7] and by the mode−mode coupling (MC) model.[8,9] In the most accepted TR model, a polymer chain feels the topological constraints exerted by neighboring chains, which are represented by a fictitious curved tube. All the models predict characteristic power law dependences of the segmental mean-squared displacement (MSD, $\langle r^2(t)\rangle$) on time. In the TR
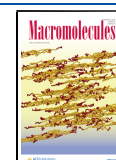
model, four power law regions (I−IV) for the MSD are predicted in succession from high to low frequencies: regimes I (Rouse dynamics), II (constrained Rouse dynamics or local reptation), and III (reptation) reflect subdiffusive motions characterized by $\langle r^2(t) \rangle \propto t^\alpha$ with $\alpha \leq 0.5$, whereas in the fourth regime (regime IV) molecules undergo Fickian diffusion ($\alpha = 1$).[10]

Sulfur curing (vulcanization) is employed in tire industry to obtain rubbers with desirable mechanical properties. The formation of sulfur bridges results in permanent cross-linking of polymer chains, which imposes geometric constraints on chain dynamics, in addition to transient physical entanglements. For entangled polymer networks, Lang and Sommer[11,12] proposed a model in which a phantom network with cross-links attached to an elastic background is considered and segmental fluctuations of chain strands between cross-links are confined within a tube determined by entanglements with neighboring chains. The chain segments slide along the tube, similarly to the case of polymer melts, but reach a constant finite value of the MSD in the long time limit. Moreover, a different distribution of fluctuation amplitudes for segments in different positions of the chain was found by computer simulations for polymer networks and polymer melts. Therefore, different mode distributions could be expected for melts and networks in the Rouse regime and entangled dynamics could be hampered in networks, also depending on cross-link density. Upon vulcanization, glassy dynamics slows down because of an increase in the molecular friction coefficient. All this considered, cross-linking strongly affects polymer elasticity and other important properties in polymer technology, such as thermal properties and the glass transition behavior.[13−20] The investigation of the effects of cross-linking on elastomer chain dynamics is therefore of interest from a fundamental point of view and for establishing relationships with macroscopic properties that are important in order to design new materials for specific applications.

Nuclear magnetic resonance (NMR) offers many versatile techniques for the characterization of dynamics in polymers. Among them, ^{1}H field-cycling (FC) NMR relaxometry allows a broad range of frequencies to be investigated.[21−23] It thereby represents an ideal tool for the characterization of polymer dynamics, which takes place over a huge range of characteristic times.[24] In fact, this technique measures the dependence on Larmor frequency (ν or $\omega = 2\pi\nu$) of the proton longitudinal relaxation rate, $R_1 = 1/T_1$ (T_1 is the longitudinal relaxation time), also referred to as nuclear magnetic relaxation dispersion (NMRD). To a fair approximation, NMRD curves reflect the spectrum of reorientational and translational dynamics of polymer segments (see the Theoretical Background) and may be analyzed to get information on both glassy and polymer dynamics.

^{1}H FC NMR relaxometry has been indeed extensively applied to study the dynamics of linear polymer melts, both below and above the entanglement limit, especially focusing on testing models on ideal polymers, that is, simple unbranched polymers in the molten state at favorable experimental temperatures.[24−36] In particular, ^{1}H FC NMR relaxometry measurements on several linear polymers have been reviewed by Kimmich and Fatkullin,[24] which, at $\omega\tau_s \ll 1$, appear to reveal an universal dispersion behavior of R_1 with characteristic power law regimes $R_1(\omega) \propto \omega^{-\gamma}$. These dispersions have been interpreted within Rouse and renormalized Rouse theories for nonentangled and entangled polymers, respectively. The [1]H R_1

dispersion behavior has been more recently reinvestigated by Rössler and co-authors.[25,27−32,35] By exploiting the frequency−temperature superposition (FTS) principle, which applies for polymers at $T \gg T_g$ (where T_g is the glass transition temperature),[37,38] R_1 data have been transformed to the susceptibility representation $\chi''(\omega) = \omega R_1(\omega)$ and master curves of $\chi''(\omega\tau_s)$ have been built (see the Theoretical Background) and interpreted in a new fashion in order to extract contributions from glassy and polymer dynamics, to investigate the crossover from simple liquid to Rouse and to entanglement dynamics as a function of M, to confirm the existence of an universal polymer dynamics, and to disentangle contributions to relaxation arising at different frequencies from reorientational and translational motions.

Notwithstanding the importance of elastomers in materials science and industrial applications and the great utility of ^{1}H FC NMR relaxometry in studying dynamics, a small number of papers have been reported in the literature concerning the investigation of chemically cross-linked polymer networks using this technique.[10,39−43] In particular, in the papers by Kariyo and Stapf, cross-linked elastomers were considered as polymer melts to which sparse fixed geometrical constraints are added, and the observed differences with respect to un-cross-linked elastomers were ascribed to a slowdown of both glassy and polymer dynamics, the motional spectrum remaining virtually unchanged.

In the present work, NMRD curves were acquired over a wide range of frequencies (0.01−35 MHz) and temperatures on three elastomers of high technical importance in the tire industry, that is, isoprene rubber (IR), butadiene rubber (BR), and styrene-co-butadiene rubber (SBR) both uncured and vulcanized under different conditions. By passing to the susceptibility representation, master curves were built, which allowed dynamics to be investigated over a broad frequency range. The τ_s correlation times, characterizing glassy dynamics, were determined for all samples at different temperatures and used to investigate the effects of the cross-linking density and cross-link type on the glass transition behavior. The contributions of polymer and glassy dynamics to the total motional spectrum were extracted and restrictions to polymer dynamics from chemical cross-links were highlighted for the different rubbers.

■ THEORETICAL BACKGROUND

For protons, longitudinal relaxation is governed by the modulation of the magnetic dipole−dipole interaction of [1]H−[1]H spin pairs by molecular motions. The interaction Hamiltonian results from the sum of all pairs of spins i,j in the sample, separated by vectors $\mathbf{r}_{ij}$. For each pair, the interaction term depends on the orientation of $\mathbf{r}_{ij}$ with respect to the magnetic field and on the distance r_{ij}. In the case of polymers, contributions to R_1 arise from both intrachain (or intrasegment) dipolar couplings, modulated by reorientations ($R_{1,intra}$), and interchain (or intersegment) couplings, modulated by both reorientational and translational dynamics ($R_{1,inter}$). Although the intrachain contribution dominates at high frequency, the interchain contribution becomes increasingly important and exceeds the intrachain one at low frequencies.[34−36]

The R_1 dispersion reflects the spectrum of motions of [1]H−[1]H spin pairs and can be expressed as a linear combination of spectral densities, $J(\omega)$. The latter is the Fourier transform

of the dipolar autocorrelation function, $C(t)$. Relaxation rate and spectral density are connected by Bloembergen−Purcell−Pound (BPP) theory through the equation[44]

$$R_1(\omega) = K[J(\omega) + 4J(2\omega)] \tag{1}$$

where K is a proportionality constant depending on the second moment of the relevant intra- or intersegment dipolar interactions.

The spectral density for the reorientations within the Kuhn segment (glassy dynamics) can be phenomenologically described by the Cole−Davidson (CD) function[45]

$$J_{CD}(\omega) = \frac{\sin[\beta_{CD} \arctan(\omega\tau_{CD})]}{\omega[1 + (\omega\tau_{CD})^2]^{\frac{\beta_{CD}}{2}}} \tag{2}$$

where $0 < \beta_{CD} \leq 1$ and the characteristic time τ_{CD} is related to τ_s by the expression $\tau_s = \beta_{CD}\tau_{CD}$.

According to Kimmich and Fatkullin,[24] glassy dynamics is mostly responsible for the decay of the dipolar autocorrelation function. As a consequence, the temperature at which T_1 reaches the minimum value (or maximum for the corresponding R_1), usually observed at high frequency in FC NMR experiments at low temperature, is predominantly determined by this component and indicates the value of τ_s via the "minimum condition" $\omega\tau_s \simeq 1$ (actually $\omega\tau_s$ ranges from ∼0.42 for $\beta_{CD} \odot 0$ to ∼0.62 for $\beta_{CD} = 1$). However, glassy dynamics covers only a restricted solid-angle range of the ^{1}H−^{1}H interdipolar vector, so that the dipolar autocorrelation function does not decay to zero. The residual correlation decays by polymer dynamics.

For polymer dynamics, dipolar translational ($C_{trans}(t)$) and rotational ($C_{rot}(t)$) autocorrelation functions can be written for $t \gg \tau_s$ as proportional to power laws of $\langle r^2(t) \rangle$. Thereby, depending on the chosen model, different power dependences of $C_{trans}(t)$ and $C_{rot}(t)$ on time and, correspondingly, of $R_{1,intra}$ and $R_{1,inter}$ on frequency are found in the different regimes.[34,35] In particular, in the TR model, $C_{rot}(t) \propto t^{-1}$, $t^{-1/4}$, and $t^{-1/2}$ in regimes I, II, and III, respectively.

On the basis of the fluctuation−dissipation theorem,[25,28,31] the spectral density, $J(\omega)$, of thermal equilibrium fluctuations of a property is related to the linear response of that property to a weak external perturbation, that is, to a susceptibility function. In particular, the imaginary part of the susceptibility is given by $\chi''(\omega) = \omega J(\omega)$. This relationship is of help in the analysis of FC NMR data and in comparisons with other techniques for the investigation of dynamics that give access to susceptibility, such as dielectric spectroscopy and rheology, as pointed out by Rössler and co-authors.[35] On the basis of eq 1, one can write

$$\omega R_1(\omega) = K[\chi''(\omega) + 2\chi''(2\omega)] \tag{3}$$

Considering 2ω to be not too different from ω, $\omega R_1(\omega) \cong 3K\tilde{\chi}''(\omega)$, where $\tilde{\chi}''(\omega)$ is the "normalized NMR susceptibility" and 3 is a normalization factor to provide an integral over $\tilde{\chi}''(\omega)$ of $\pi/2$. Moreover, a (non-normalized) total FC NMR susceptibility $\chi''_{DD}(\omega) = \omega R_1(\omega)$ has been introduced to analyze FC NMR data.

Assuming the validity of the FTS principle, master curves of $\chi''(\omega\tau_s)$ can be built as a function of frequency reduced by the correlation time for glassy dynamics by shifting $\chi''(\omega)$ curves collected at different temperatures along the frequency axis until they overlap. Under the assumption that K does not

change significantly with temperature, master curves can also be obtained for $\chi''_{DD}(\omega)$.

Considering that polymer and glassy dynamics are statistically independent and well separated in time, the FC NMR susceptibility $\chi''_{DD}(\omega)$, in the following simply indicated as $\chi''(\omega)$, can be expressed as the sum of glassy and polymer contributions

$$\chi''(\omega) = (1 - f)\chi''_{glass}(\omega) + f\chi''_{pol}(\omega) \tag{4}$$

f represents the fractional contribution of polymer dynamics to the total spectrum of motions and is given by

$$f = \frac{\int_{-\infty}^{\infty} \chi''_{pol}(\omega) d\ln\omega}{\int_{-\infty}^{\infty} \chi''(\omega) d\ln\omega} \tag{5}$$

f is related to the dynamic order parameter S ($S = \sqrt{f}$), which is a measure of the spatial restrictions imposed on segmental motions by chain connectivity and entanglements. However, being derived from a ^{1}H−^{1}H dipolar autocorrelation function, its value also depends on the angles (θ_{ij}) formed between the internuclear vectors of ^{1}H−^{1}H spin pairs and the contour of the polymer chain ($S = 1/2 (3\cos^2\theta_{ij} - 1) S_{chain}$, where S_{chain} is the chain order parameter).

Because the total spectrum of motions is dominated by glassy dynamics, the spectrum of polymer dynamics $\chi''_{pol}(\omega)$ can be correctly interpreted only after subtracting $\chi''_{glass}(\omega)$ from $\chi''(\omega)$. $\chi''_{glass}(\omega)$ can be determined experimentally as the total $\chi''(\omega)$ for polymers with very small molar mass, which do not undergo Rouse or reptation polymer dynamics. Furthermore, it can be theoretically expressed as a function of the CD spectral density (eq 2) as

$$\chi''_{glass}(\omega) = \omega K_{CD}[J_{CD}(\omega) + 4J_{CD}(2\omega)] \tag{6}$$

$\chi''_{glass}(\omega)$ coincides with $\chi''(\omega)$ for frequencies larger than $\approx 1/\tau_s$. Therefore, τ_s values can be determined by fitting the high-frequency branch of the $\chi''(\omega)$ curves, ascribable to the sole glassy dynamics, to eq 6 with $J_{CD}(\omega)$ as in eq 2.

τ_s correlation times exhibit non-Arrhenius temperature dependence, as expected for the structural relaxation. The Vogel−Fulcher−Tammann (VFT) empirical equation[37]

$$\tau_s = \tau_0 \exp\left(\frac{DT_0}{T - T_0}\right) \tag{7}$$

is generally used to describe these data, where τ_0 is a pre-exponential factor, T_0 is the temperature at which the correlation time diverges to infinity, and D is a fragility factor. The glass transition temperature T_g can therefore be determined as the temperature at which τ_s is 100 s.[46] A measure of polymer fragility, that is, of the rapidity with which glassy dynamics slows down on cooling the polymer toward the glass transition, can be given by determining the fragility index m defined as

$$m = -\left.\frac{d\mathrm{Log}\tau_s(T/T_g)}{d(T/T_g)}\right|_{T_g} \tag{8}$$

Blochowicz et al. showed that the VFT equation can be recast in terms of m and T_g to give[47]

Table 1. Vulcanization Conditions of the Investigated Rubbers, Cross-Link Density Values Obtained by Equilibrium Swelling Experiments, and T_g Values Determined by DSC

sample	sulfur (phr)	TBBS (phr)	T_{vulc} (°C)	$1/M_c$ (10^{-5} mol/g)	T_g (K)
IR_S1_150	1	3	150	3.53	211
IR_S2_150	2	3	150	5.07	213
IR_S3_150	3	3	150	6.25	214
BR_S1_150	1	3	150	5.72	169
BR_S2_150	2	3	150	7.93	169
BR_S3_150	3	3	150	8.13	171
SBR_S1_150	1	3	150	2.49	230
SBR_S2_150	2	3	150	3.77	234
SBR_S3_150	3	3	150	5.12	235
IR_29	1	3	170	3.20	211
IR_60	2	2	170	3.25	213
IR_80	3	1	170	3.00	213
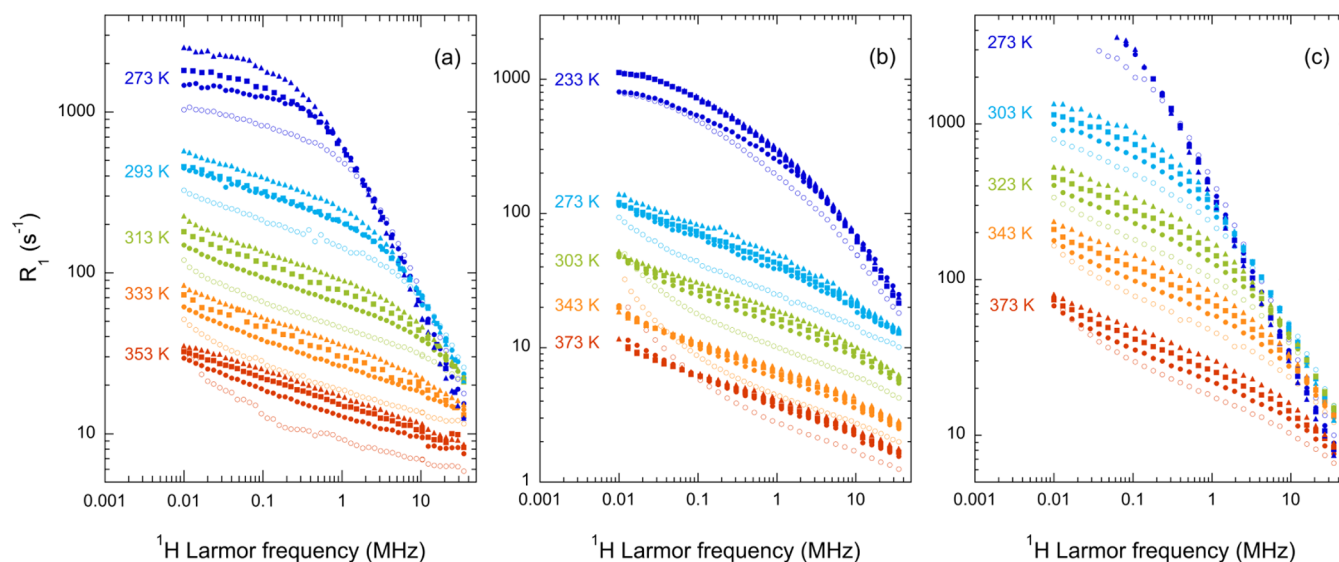
Figure 1. ^{1}H NMRD curves acquired at the indicated temperatures on samples: (a) IR (empty circles), IR_S1_150 (full circles), IR_S2_150 (full squares), and IR_S3_150 (full triangles); (b) BR (empty circles), BR_S1_150 (full circles), BR_S2_150 (full squares), and BR_S3_150 (full triangles); and (c) SBR (empty circles), SBR_S1_150 (full circles), SBR_S2_150 (full squares), and SBR_S3_150 (full triangles).

$$\text{Log}\left[\frac{\tau_s(T)}{\tau_0}\right] = \frac{\text{Log}^2\left[\frac{\tau_s(T_g)}{\tau_0}\right]}{m\left(\frac{T}{T_g} - 1\right) + \text{Log}\left[\frac{\tau_s(T_g)}{\tau_0}\right]} \qquad (9)$$

On the basis of this equation, polymers with same τ_0 and m show a superposition of $\text{Log}\tau_s$ versus $(T/T_g - 1)$ curves.

■ MATERIALS AND METHODS

Materials. All samples were provided by Pirelli Tyre SpA (Milano, Italy). IR (cis-1,4-polyisoprene, ≥96% cis, $M_w = 1.49 \times 10^6$ g/mol, and $M_n = 8.41 \times 10^5$ g/mol), BR (cis-1,4-polybutadiene, 97.5% cis, $M_w = 3.57 \times 10^5$ g/mol, and $M_n = 1.15 \times 10^5$ g/mol), or SBR (poly(styrene-co-butadiene), 25% styrene, vinyl content on the dienic portion 25%, $M_w = 2.50 \times 10^5$ g/mol, and $M_n = 1.52 \times 10^5$ g/mol) was used as the base for the cross-linked rubbers.

For the preparation of samples denominated IR_Sphr_150, BR_Sphr_150, and SBR_Sphr_150, IR, BR, and SBR were mixed with 3 phr (parts per hundred rubber) of ZnO, 2 phr of stearic acid, 1, 2, or 3 phr of sulfur, 3 phr of N-tert-butyl-2-benzothiazole sulfenamide (TBBS) as an accelerator, and 2 phr of N-(1,3-dimethylbutyl)-N′-phenyl-p-phenylenediamine (6PPD) as an antioxidant and were vulcanized into sheets of 1 mm thickness at T_{vulc} = 150 °C. Three vulcanized IR-based samples were also prepared with approximately

the same cross-link density but with a different content of mono- (C−S−C), di- (C−S−S−C), and polysulfidic (C−S$_x$−C, x ≥ 3) bridges. To this aim, IR was mixed with 3 phr of ZnO, 2 phr of stearic acid, 2 phr of 6PPD, and appropriate amounts of sulfur and other additives (Table 1) and vulcanized into sheets of 1 mm thickness at T_{vulc} = 170 °C. These samples are indicated as IR_29, IR_60, and IR_80, with the number indicating the percentage of cross-links constituted by polysulfidic bridges, determined using the thiol-amine analysis.[48] Samples vulcanized at the maximum degree of cross-linking were considered for FC NMR measurements.

Cross-link density, defined as $1/M_c$, where M_c is the average molar mass between two adjacent cross-links, was determined from equilibrium swelling data in toluene using the Flory−Rehner equation;[48] $1/M_c$ values of all vulcanized elastomers are reported in Table 1.

Glass transition temperatures (T_g) were determined by differential scanning calorimetry (DSC) using a DSC Mettler-Toledo 822e instrument. Thermal cycles between 148 and 323 K were performed for BR-based samples, while for IR- and SBR-based samples, thermal cycles were performed from 183 to 323 K. The cooling/heating rate was 10 K/min. T_g was determined as the intersection point of the two tangents to the DSC curve at the endothermic step. For uncured IR, BR, and SBR, T_g was 208, 167, and 225 (±1) K, respectively; T_g values of vulcanized rubbers are reported in Table 1.

^{1}H FC NMR Relaxometry Measurements. ^{1}H R_1 values were measured at different temperatures in the 0.01−35 MHz Larmor frequency range using a Spin Master FFC-2000 FC NMR relaxometer (Stelar srl, Mede, Italy). The prepolarized and non-prepolarized pulse sequences[21,22] were used below and above 12 MHz, respectively. The polarizing and detection frequencies were 25.0 and 16.3 MHz, respectively. The switching time was 3 ms and the 90° pulse duration was 9.8 μs. A single scan was acquired. All the other experimental parameters were optimized for each measurement. All the ^{1}H magnetization curves *versus* time were monoexponential within the experimental error and the errors on R_1 were always lower than 2%. For measurements, samples were cut into small pieces and introduced in a 10 mm diameter glass tube. The temperature was controlled within ±0.1 °C with a Stelar VTC90 variable temperature controller.

Data Analysis. Fittings of the susceptibility curves were performed using the least-squares minimization procedure implemented in the Fitteia environment.[49,50] The spectral decomposition of the susceptibility master curves and the determination of power law exponents were carried out using purposely written programs in the Mathematica environment.[51]

■ RESULTS AND DISCUSSION

NMRD and NMR Susceptibility Curves as a Function of Temperature and Cross-Linking. ^{1}H FC NMR relaxometry experiments were performed at different temperatures on uncross-linked and cross-linked IR (253−373 K), BR (213−373 K), and SBR (273−373 K) samples (Table 1); a selection of NMRD curves is reported in Figure 1, while NMR susceptibility ($\chi''(\omega) = \omega R_1(\omega)$) curves are shown in Figure S1.

Uncured IR shows NMRD curves with three different power law dependences of R_1 on Larmor frequency ($R_1(\omega) \propto \omega^{-\gamma}$), depending on the temperature (Figure 1a). At all the investigated temperatures, a regime with $\gamma \cong 0.16$ is observed. For $T = 303$ and 313 K, a regime characterized by $\gamma \cong 0.51$ is observed at high frequencies; γ progressively increases by decreasing the temperature, reaching values of 1.1 at the lowest temperatures. For $T \geq 303$ K, a small region with $\gamma \cong 0.37$ (determinable only for the highest temperatures) is found at low frequencies. The crossover points between regimes are shifted toward higher frequencies with increasing temperature.

The observed exponents are similar to those determined by other authors for polyisoprene with molar mass above the entanglement limit[10,40,41] and attributed by Kimmich and Fatkullin to regimes I (high mode number limit; intrasegment dipolar interaction; $\gamma = 0.5 \pm 0.05$), II (low mode number limit; intrasegment dipolar interaction; $\gamma = 0.25 \pm 0.05$), and III (low mode number limit; intersegment dipolar interaction; $\gamma = 0.44 \pm 0.05$) of renormalized Rouse theory.[24] The anomalous value of γ found for IR in regime II (0.16) was already pointed out and discussed in the literature by several research groups (*vide infra*).[29,52] In terms of the TR model, which we will refer to hereafter, the regime with $\gamma \cong 0.16$ is ascribable to the Rouse regime (regime I, $\gamma = 0$), while that with $\gamma \cong 0.37$ is ascribable to an incipient constrained Rouse regime (regime II, $\gamma = 0.75$), as better discussed below. The increase in the exponent observed on cooling at high frequencies and low temperature results from the overlap of the time scales of reorientations within the Kuhn segments in the glassy dynamics regime (regime 0) and motions of the Kuhn segments themselves in the incipient regime I. In fact, at the lowest temperatures, the high-frequency region is dominated by glassy dynamics; the maximum observed for R_1 on changing the temperature is due to the matching

between the Larmor frequency and the frequency of glassy dynamics (*i.e.*, the condition $\omega\tau_s \cong 1$ is satisfied).

The vulcanized IR-based samples show NMRD curves analogous to those of uncured IR in regimes I and 0 (Figure 1a), whereas power law dependences typical of regime II are never detected for them, despite the high temperatures investigated (up to 383 K). The values of γ are equal to 0.17−0.18 in regime I at all the temperatures. Higher R_1 values in all frequency regions at each temperature are observed for cross-linked rubbers with respect to IR. This behavior indicates a progressive slowdown of motions with increasing cross-link density of the rubbers, analogous to that observed for IR on decreasing the temperature. A similar behavior was observed by Stapf and co-workers in natural rubber, an elastomer essentially made of polyisoprene.[40,41] Moreover, for the sulfur-cured samples, the temperatures at the R_1 maxima are higher than those of uncured IR, indicating the slowing down of glassy dynamics with increasing cross-link density. The matching between the glassy dynamics time scale and the experimental Larmor frequency ($\omega\tau_s \cong 1$) gives rise to a maximum of the $\chi''(\omega)$ curves for $T \leq 273$ K, the maximum shifting to lower frequencies with increasing cross-link density. The power laws found for the R_1 dispersions are reflected in $\chi''(\omega) \propto \omega^{1-\gamma}$ dependences (Figure S1a).

A selection of NMRD and NMR susceptibility curves of BR-based samples is reported in Figures 1b and S1b, respectively. Between 213 and 233 K, uncured BR shows curves mainly arising from glassy dynamics and polymer dynamics in regime I of the TR model. At the lowest temperatures, polymer dynamics in regime I occurs on a time scale overlapping that of glassy dynamics; the resulting effective γ is about 1.1. In regime I, NMRD curves follow a power law with $\gamma = 0.24−0.25$. This regime is found to dominate the NMRD curves between 253 and 303 K. For $T \geq 283$ K, a more pronounced dispersion region is observed at low frequencies, with $\gamma \cong 0.65$, ascribable to regime II of TR. By increasing the temperature, the crossover points between regimes are shifted toward higher frequencies. These findings are in accordance with those reported in the literature for high-molar mass polybutadiene melts.[39,53] NMRD and susceptibility curves analogous to those of uncured BR are observed for the sulfur-cured BR samples, with γ values similar to those of regimes I and 0. BR_S1_150, the rubber with the lowest cross-link density, additionally shows a more pronounced dispersion below 30 kHz at $T \geq 363$ K. The R_1 values at each investigated temperature increase with increasing cross-link density. A similar behavior was reported by Kariyo and Stapf for rubbers obtained by vulcanization of polybutadiene at 160 °C with 1, 2, 3, and 4 phr of sulfur.[42]

Selected FC NMR data acquired on uncross-linked and cross-linked SBR are shown in Figures 1c and S1c. At $T = 273$ K, NMRD and corresponding susceptibility curves essentially due to glassy dynamics are observed for uncured SBR. By increasing the temperature, regimes I and II of the TR model are found at lower frequencies with regime II being observed at very low frequencies only for the highest investigated temperatures ($T \geq 363$ K). In the high-frequency regime, R_1 shows a maximum as a function of temperature because of the matching of the condition $\omega\tau_s \cong 1$ for the glassy dynamics; correspondingly, maxima are observed in the $\chi''(\omega)$ curves. The γ values are 0.23−0.26 in regime I and $\cong 0.48$ in regime II. The vulcanized SBR-based samples show NMRD and susceptibility curves similar to those of uncured SBR in
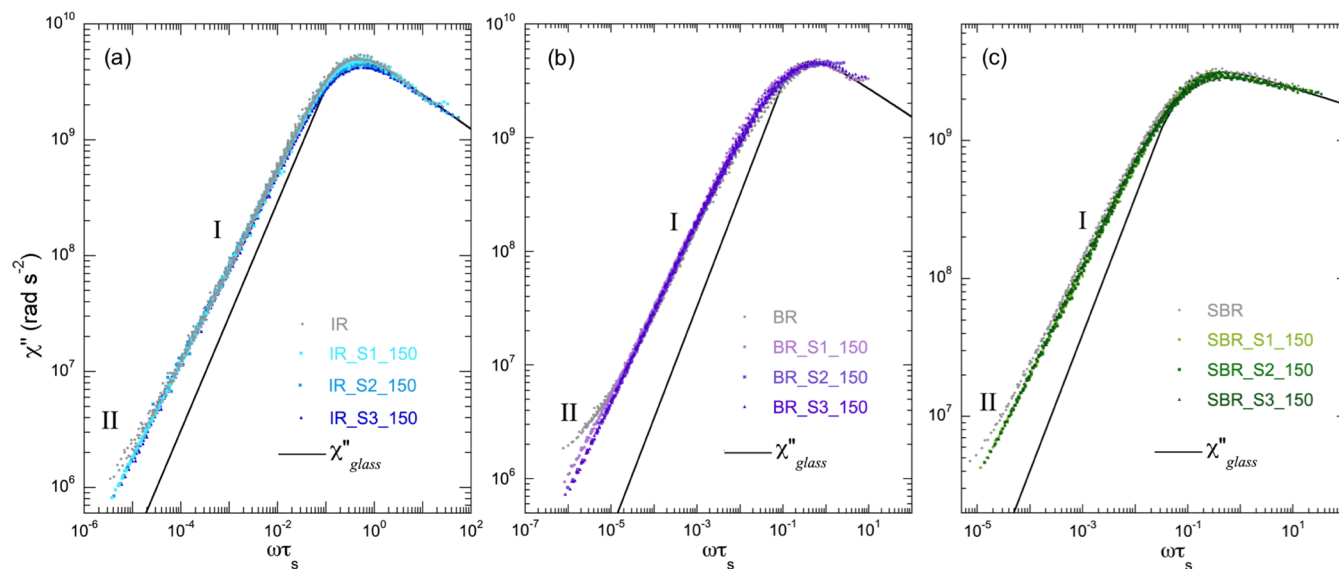
Figure 2. $\chi''(\omega\tau_s)$ master curves for: (a) IR, IR_S1_150, IR_S2_150, and IR_S3_150; (b) BR, BR_S1_150, BR_S2_150, and BR_S3_150; and (c) SBR, SBR_S1_150, SBR_S2_150, SBR_S3_150. Black lines represent the curves used to fit the $\chi''(\omega\tau_s)$ master curves at high frequency to eq 6 with a Cole−Davidson spectral density function (eq 2) for IR, BR, and SBR.
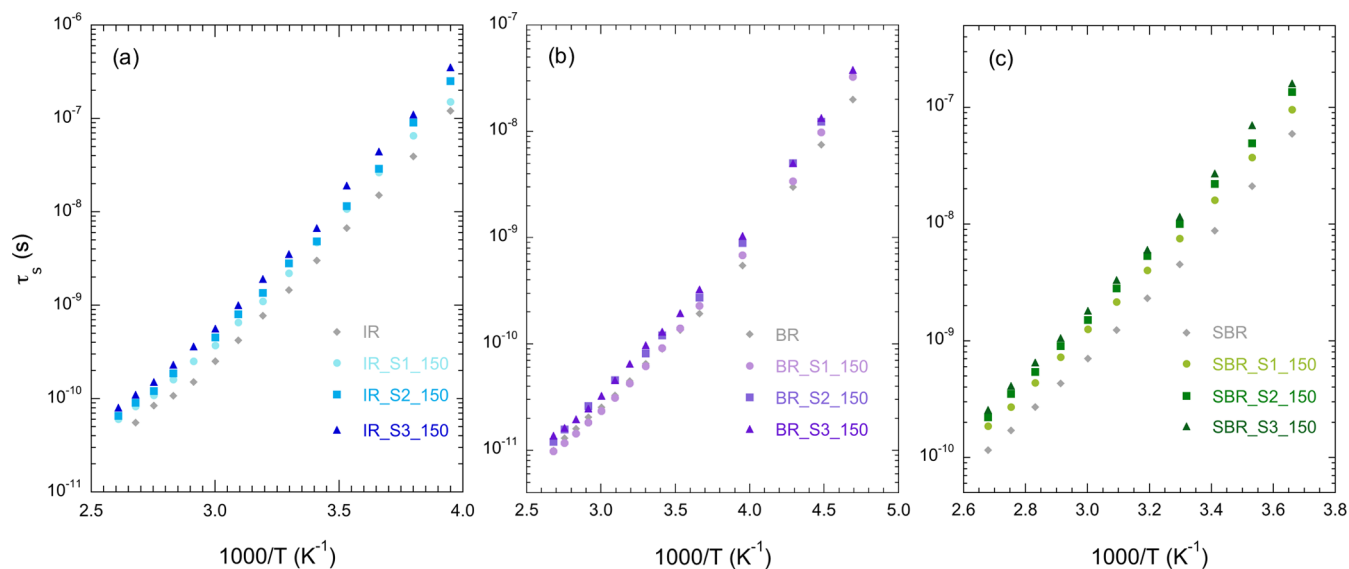

Figure 3. Correlation times for glassy dynamics, τ_s, vs $1000/T$ for: (a) IR, IR_S1_150, IR_S2_150, and IR_S3_150; (b) BR, BR_S1_150, BR_S2_150, and BR_S3_150; (c) SBR, SBR_S1_150, SBR_S2_150, and SBR_S3_150.

regimes I and 0. The maxima of R_1 as a function of temperature at high frequencies occur at higher temperatures for samples with higher cross-link density. Correspondingly, the maxima of the $\chi''(\omega)$ curves observed at the lower temperatures are shifted to lower frequencies (Figure S1c).

In order to better discern the effect of sulfur bridges with different lengths on dynamics in IR-based rubbers with similar cross-link densities, ^{1}H NMRD curves were also acquired in the 263−363 K temperature range on samples IR_29, IR_60, and IR_80, characterized by an increasing content of polysulfidic bridges; representative results are shown in Figure S2. NMRD and NMR susceptibility curves are similar to those of the other IR-based samples, showing characteristic features of glassy dynamics at high frequencies and lower temperatures and of regime I of TR at low frequencies and higher temperatures. By increasing the content of polysulfidic bridges,

a small increase in R_1 is observed at all temperatures in the NMRD curves, while a slight shift to lower frequencies is found for the maxima in the susceptibility curves. These features indicate a slowdown of glassy dynamics in rubbers with a higher content of polysulfidic bridges.

NMR Susceptibility Master Curves. NMR susceptibility, $\chi''(\omega)$, curves obtained for the different samples at the investigated temperatures (a selection is shown in Figures S1 and S2b) were employed to build $\chi''(\omega\tau_s)$ master curves by shifting along the frequency axis by the correlation times for glassy dynamics, τ_s. For the $\chi''(\omega)$ curves collected at the lowest temperatures, clearly showing the maximum and both low- and high-frequency branches, the high-frequency branch was fitted to eq 6 with the Cole−Davidson spectral density (eq 2). In particular, for samples in the IR series, the high-frequency branch of $\chi''(\omega)$ curves at 263 and 273 K was fitted
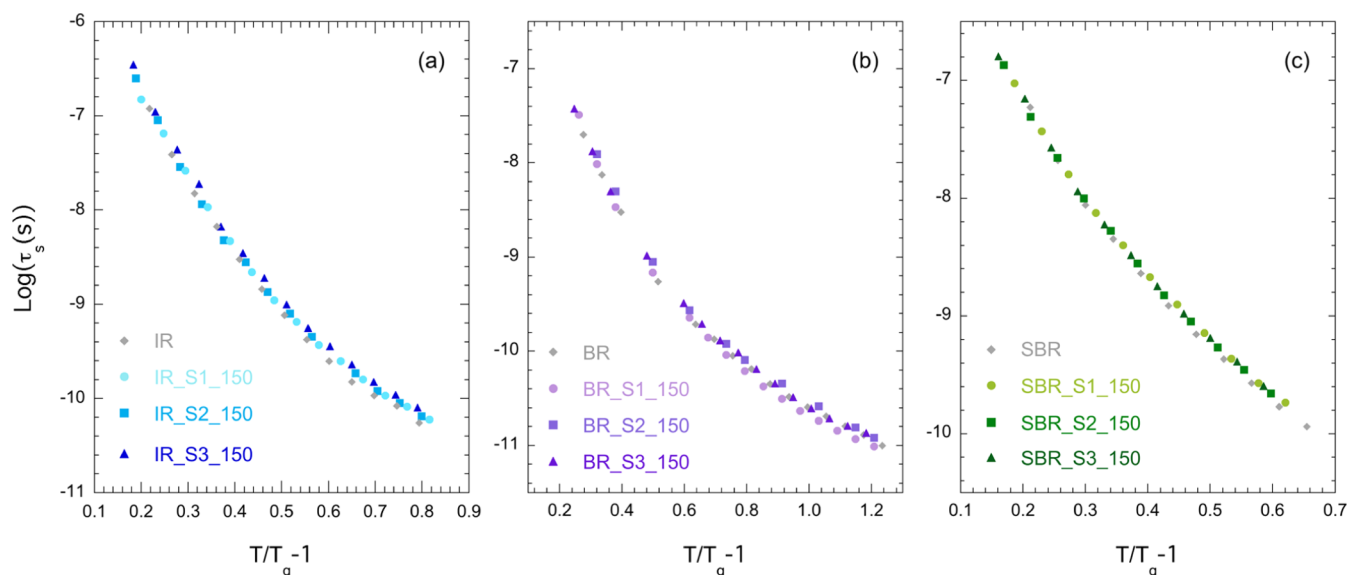
Figure 4. Logτ_s *vs* $(T/T_g - 1)$ for: (a) IR, IR_S1_150, IR_S2_150, and IR_S3_150; (b) BR, BR_S1_150, BR_S2_150, and BR_S3_150; and (c) SBR, SBR_S1_150, SBR_S2_150, and SBR_S3_150; T_g was determined by DSC measurements.

and good fittings were obtained with $\beta_{CD} = 0.30$. In the case of BR-based samples, the high-frequency flank of the susceptibility curves at $T \leq 223$ K was fitted with $\beta_{CD} = 0.25$, whereas the best fit value of β_{CD} found for all SBR-based samples at low temperatures $(T \leq 283$ K$)$ was 0.12. We then plotted the susceptibility curves as a function of $\omega\tau_s$, being $\tau_s = \beta_{CD}\tau_{CD}$. The $\chi''(\omega)$ curves at higher temperatures, only showing the low-frequency branch, were shifted solely along the frequency axis until they overlapped those at lower temperatures, taken as a reference; τ_s values were determined from the shift factors. The $\chi''(\omega\tau_s)$ master curves built for the different samples with the above-described procedure are shown in Figures 2 and S3, while the determined τ_s values are reported in Figures 3 and S4a.

The $\chi''(\omega\tau_s)$ master curves obtained for the investigated samples cover wide ranges of frequency (7 orders of magnitude of $\omega\tau_s$, almost 6 at $\omega\tau_s < 1$) and amplitude (about 4 orders of magnitude) and show characteristic shapes, reflecting the hierarchy of motions of polymer chains in the different regimes: at high reduced frequency, glassy dynamics dominates, whereas for $\omega\tau_s < 10^{-1}$, the contribution of polymer dynamics becomes progressively more important.

Almost identical master curves were obtained for all the sulfur-cured IR rubbers, which differ from those of uncured IR only at very low frequency, where regime II of the TR model is observed for the latter sample (Figure 2a). The master curve obtained for uncured IR is quite similar to that reported in the literature for samples of linear high-molar mass polyisoprene.[29,30,54] The $\chi''(\omega\tau_s)$ curve of uncured BR results from the contribution of glassy dynamics and polymer dynamics in regimes I and II, in analogy to that reported in the literature for linear high-molar mass polybutadiene samples.[25,27,29–31] On the other hand, the $\chi''(\omega\tau_s)$ curves of cross-linked BR-based rubbers show the contribution from glassy dynamics and regime I of polymer dynamics. A deviation from the slope of regime I is observed at the lowest $\omega\tau_s$ values for BR_S1_150 (Figure 2b), as already evidenced by the NMRD and susceptibility curves at the highest temperatures. Master curves are very similar for all the vulcanized SBR-based rubbers, which, however, differ from those of uncured SBR at low

frequencies, where regime II is found for the latter sample (Figure 2c). The differences between cross-linked and corresponding uncross-linked elastomers can be better highlighted by dividing $\chi''(\omega\tau_s)$ curves by the reduced frequency $\omega\tau_s$, as shown in Figure S5; in this way, master curves of $R_1(\omega\tau_s)/\tau_s$ are obtained, which can be considered as a sort of spectral density $(J(\omega\tau_s) = \chi''(\omega\tau_s)/\omega\tau_s)$ master curves.

By applying the derivative method described in refs 32 and 55, the exponents of the power law dependences of $\chi''(\omega\tau_s)$ on the reduced frequency were determined for all samples. Exponent values of 0.85 ± 0.10, 0.78 ± 0.10, and 0.75 ± 0.05 were found in regime I for uncured IR, BR, and SBR, respectively. Considering the rotational dynamics in the framework of TR theory, the exponent in regime I arising from Rouse dynamics should be 1, although values close to ours were found for entangled polymer melts both in experimental studies by FC NMR[28,32] and DQ NMR[55,56] and in computer simulations[57,58] and ascribed to a reduced number of Rouse modes due to chain local stiffness. In regime II, exponent values of ~0.66, 0.30, and 0.51 were determined for uncross-linked IR, BR, and SBR, respectively, which are higher than those predicted by the TR model for rotations in the constrained Rouse regime (0.25). Although the contribution of interchain dipolar interactions cannot be excluded at low frequencies, this discrepancy can be mainly ascribed to the fact that a restricted frequency range was investigated for regime II because of technical limitations.

Cross-linked elastomers show exponent values in the same ranges of those determined for the corresponding uncured ones in regime I. The lack of a deviation from this power law dependence at low reduced frequencies indicates that geometrical constraints introduced by vulcanization hamper long-range coherent chain motions, the chain dynamics remaining limited to local motions in the free Rouse regime.

Effects of Cross-Linking on Glassy Dynamics. Within each series of elastomers, the cross-link density, as determined from equilibrium swelling experiments,[48] increases linearly with the sulfur amount used in vulcanization (Figure S6), with intercept values of 2.2×10^{-5}, 4.8×10^{-5}, and 1.2×10^{-5} mol/ g for IR-, BR-, and SBR-based rubbers, respectively; these

values represent the density of trapped entanglements, not relaxed under swelling conditions, which are considerably larger for BR-based samples. By comparing the M_c values of cross-linked rubbers (Table 1) with the corresponding M_e values determined from the plateau modulus for uncured elastomers with a similar microstructure (3120 g/mol for IR,[59] 2350 g/mol for BR,[59] and 3000 g/mol for SBR[37]) it can be inferred that the investigated rubbers are moderately cross-linked.

As already observed from NMRD and NMR susceptibility curves, a slowdown of glassy dynamics occurs for all the investigated elastomers after vulcanization, which increases with the increasing amount of sulfur and cross-link density. Restrictions imposed by the network junctions reduce the configurational freedom of the chains and increase the local friction. This effect is more quantitatively described by the trends of τ_s reported in Figure 3. Within each series of elastomers, τ_s values progressively increase with increasing cross-link density at the same temperature, in analogy to what observed by Hernández *et al.* for natural rubber using broadband dielectric spectroscopy.[20] Moreover, slightly longer τ_s values were found for IR samples showing a very similar cross-link density but a higher fraction of polysulfidic links (Figure S4a), indicating an effect of the cross-link type on glassy dynamics. These results are in qualitative agreement with the increase in T_g values measured by DSC (see the Materials and Methods section) by increasing the cross-link density or the fraction of polysulfidic links. For uncured IR and BR, the τ_s values are consistent with those previously reported in the literature for linear polyisoprene[10,30] and polybutadiene[25−27] samples with $M > M_e$.

For all samples, τ_s shows a non-Arrhenius temperature dependence as expected for glassy dynamics. Unfortunately, the limited range of temperature investigated hampered a robust analysis of τ_s in terms of the VFT equation (eq 7) and, thereby, the determination of dynamic T_g and the fragility index for the elastomers. By considering the static T_g determined by DSC, plots of Logτ_s *versus* $(T/T_g - 1)$, reported in Figures 4 and S4b, show a good superposition of curves for uncross-linked and cross-linked elastomers for IR- and BR-based samples; the superposition is almost perfect for elastomers of the SBR series. Slight deviations in Logτ_s *versus* $(T/T_g - 1)$ curves for vulcanized and uncured elastomers can be accounted for by possible errors in determining T_g and τ_s and on a different effect of cross-links on static and dynamic T_g. All this considered, these results indicate that if τ_0 remains unchanged, vulcanization does not appreciably affect polymer fragility (see eq 9), in agreement with results on other cross-linked polymers with relatively low cross-link densities.[14,15,17]

A linear relationship was found between T_g determined by DSC and $1/M_c$ values for all sulfur-cured rubbers (Figure 5) with slopes of $(1.1 \pm 0.1) \times 10^5$, $(0.5 \pm 0.5) \times 10^5$, and $(1.9 \pm 0.7) \times 10^5$ K·g/mol and intercepts of 207 ± 1, 166 ± 5, and 226 ± 3 K, quite close to the T_g of the corresponding uncured elastomers, for IR-, BR-, and SBR-based rubbers, respectively. The observed linear trends are in agreement with the literature,[60−65] and the slope values are in the order of those reported for other polymers.[61,64,65]

An increase in T_g was also found for vulcanized IR-based rubbers with a higher percentage of polysulfidic bridges and a very similar cross-link density (Table 1). In fact, not only the cross-link density but also the cross-link type and the presence of sulfur-polymer or curative-polymer adducts can affect the
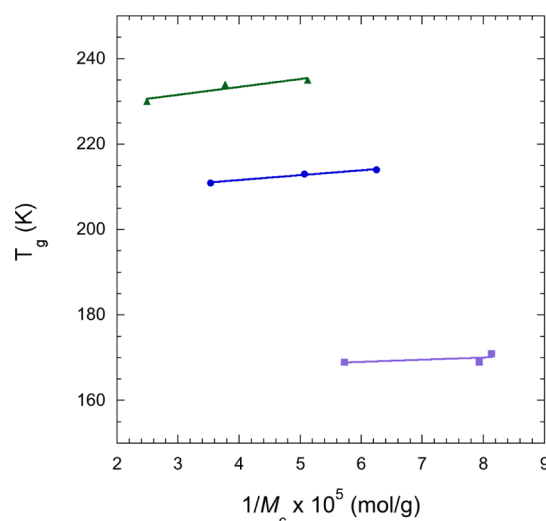

Figure 5. T_g *vs* cross-link density ($1/M_c$) for IR- (blue), BR- (purple), and SBR-based (green) rubbers.

glassy dynamics of vulcanized elastomers.[13,20,61,64,65] In particular, polysulfidic cross-links and cyclic sulfide structures, favored when vulcanization is carried out at higher sulfur/accelerant ratios, have a more profound effect on T_g than monosulfidic cross-links because they restrict the reorientation possibilities of polymer chains. On the other hand, when present in large amounts and endowed with a bulky and inflexible structure, accelerants considerably stiffen polymer chains by hampering their reorientations and/or forming transient cross-links by intermolecular interactions. In our case, because a low-molecular weight accelerant is used (TBBS) and the sulfur/accelerant ratio increases with the percentage of polysulfidic cross-links in our samples, the observed effect is ascribed to polysulfidic cross-links and, possibly, cyclic sulfide structures.

Effects of Cross-Linking on Polymer Dynamics. In order to inspect in more detail the effect of cross-linking on the dynamics of the polymer chains, the spectra due to the sole polymer dynamics, called from now on "polymer spectra", were singled out from the susceptibility master curves shown in Figure 2, following a spectral decomposition procedure similar to that described in the previous literature.[25] As shown in Figure S7 for uncured IR, BR, and SBR, the polymer spectra ($\chi''_{pol}(\omega\tau_s)$) were obtained by subtracting from each $\chi''(\omega\tau_s)$ master curve the contribution of glassy dynamics ($\chi''_{glass}(\omega\tau_s)$), described using a Cole−Davidson function, under the assumption of statistical independence and time-scale separation between glassy and polymer dynamics, such that eq 4 holds true. Moreover, the contribution of polymer dynamics at high frequencies ($\omega \gtrsim 1/\tau_s$) was assumed to be negligible, so that the high-frequency branch of $\chi''(\omega\tau_s)$ was practically coincident with $\chi''_{glass}(\omega\tau_s)$. This procedure allowed the relaxation strength of polymer dynamics, f, to be calculated on the basis of eq 5. Notably, although a similar approach was previously used for disentangling glassy and polymer spectra of polyisoprene, polybutadiene, and polydimethylsiloxane melts,[25,27,29] to the best of our knowledge, it is here applied for the first time to SBR and to cross-linked elastomers.

The polymer spectra, normalized to provide an integral equal to $\pi/2$, $\tilde{\chi}''_{pol}(\omega\tau_s)$, are shown in Figure 6 for a representative selection of samples. For uncured IR, BR, and SBR (Figure 6a), similar power law dependences of $\tilde{\chi}''_{pol}(\omega\tau_s)$
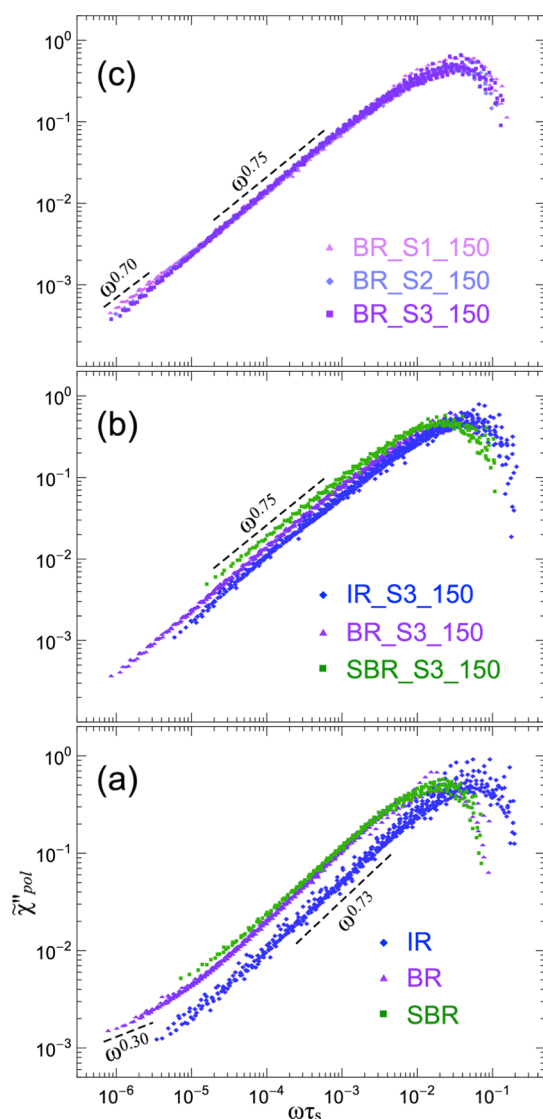
Figure 6. Normalized polymer spectra $\tilde{\chi}''_{pol}(\omega\tau_s)$ of: (a) uncured IR, BR, and SBR; (b) IR_S3_150, BR_S3_150, and SBR_S3_150 rubbers; and (c) BR_S1_150, BR_S2_150, and BR_S3_150 rubbers. Each spectrum was normalized to provide an integral equal to $\pi/2$, multiplying $\chi''_{pol}(\omega\tau_s)$ by the factor $\pi/(2fI)$,[27] where I stands for the integrated intensity of $\chi''(\omega\tau_s)$. Dashed lines indicate the power law dependences recognized for regimes I and II with the reported values of the exponent.

on reduced frequency are observed. In particular, regime I (with power law exponents between 0.70 and 0.75) and an incipient regime II (with power law exponents between 0.30 and 0.60) of the TR model can be recognized at intermediate and low reduced frequencies, respectively, while a maximum is observed at high frequency, which signs the cut off of the polymer spectrum. The exponents determined from the polymer spectra are similar but not equal to those found from the total NMRD and susceptibility curves, indicating that the contribution of glassy dynamics to ^{1}H T_1 relaxation at low frequencies is not completely negligible. As expected, the major deviations are observed for IR-based samples, for which the lowest values of f are found (*vide infra*). These results are in agreement with those previously obtained for polyisoprene and polybutadiene melts.[29]

Sulfur-cured IR-, BR-, and SBR-based elastomers show polymer spectra with a frequency dependence typical of regime I down to the lowest explored frequencies, with power law exponents of 0.75 ± 0.05 for rubbers of the BR and IR series and of 0.70 ± 0.03 for those of the SBR one, similar to those found for the corresponding uncured elastomers (Figure 6b). A slight decrease in the slope at low reduced frequencies is only observed for BR_S1_150, suggesting that longer range motions can occur in rubbers with low cross-link densities when temperature is far above T_g.

The values of f obtained for all the samples studied here, reported in Table 2, range between 0.05 and 0.14

Table 2. Relaxation Strength (f) of Polymer Dynamics Determined by the Spectral Decomposition of the NMR Susceptibility Master Curves of the Investigated Samples

sample	f
IR	0.05 ± 0.01
IR_S1_150	0.06 ± 0.01
IR_S2_150	0.06 ± 0.01
IR_S3_150	0.05 ± 0.01
BR	0.10 ± 0.02
BR_S1_150	0.13 ± 0.02
BR_S2_150	0.14 ± 0.02
BR_S3_150	0.12 ± 0.02
SBR	0.07 ± 0.02
SBR_S1_150	0.07 ± 0.02
SBR_S2_150	0.06 ± 0.02
SBR_S3_150	0.07 ± 0.02

(corresponding to values of the dynamic order parameter S between 0.22 and 0.37), confirming that the contribution of polymer dynamics is only a very small fraction of the total spectrum of motions. Although according to Kimmich and Fatkullin f should be 10^{-3} to 10^{-2}, values similar to ours were also found by Rössler and co-workers for linear polymers with $M > M_e$.[27,29,30] The smaller value of f obtained for IR with respect to BR and SBR elastomers can be explained with the absence in polyisoprene of a spin pair along the double bond, for which the orientation of the internuclear vector, closer to the contour of the chain, results in a higher value of the dynamic order parameter S (see the Theoretical Background). These results agree with those obtained by Herrmann *et al.* and Kariyo *et al.* for polyisoprene and polybutadiene polymer melts.[25,27,29] The values of f do not significantly change in passing from the uncured elastomers to the corresponding vulcanized ones, and no clear dependence on cross-link density is found. This can be due to the fact that f, as the corresponding dynamic order parameter S, depends on both free Rouse and entangled dynamics, at variance with the dynamic order parameter S_e measured by double quantum (DQ) NMR experiments,[66,67] which contains the sole contribution of entangled dynamics and represents only a small fraction (less than 10%) of S.[27] As a consequence, the increase in S_e, usually observed by DQ NMR experiments by increasing the cross-link density, could not be detected by our approach because it is in the order of the experimental error on S. The different sensitivity and precision of the FC NMR and DQ NMR approaches are inherent in the measured observables. Although R_1 arises from the fluctuations of the dipolar interaction and S is derived indirectly as the difference between the whole spectral density and the strongly

dominating contribution of glassy dynamics, in DQ NMR experiments, the residual dipolar interaction at a given time is measured directly in the time domain.[55,68]

CONCLUSIONS

Glassy and polymer dynamics were investigated on IR, BR, and SBR, three elastomers of technological interest for the tire industry, both uncured and cross-linked by sulfur curing under different conditions. ^{1}H FC NMR relaxometry measurements over a wide range of temperatures and frequencies, combined on the basis of the FTS principle, allowed dynamics to be carefully investigated over a quite broad time scale, ranging from local segmental motions within the Kuhn segment to chain dynamics within the constraints imposed by entanglements and sulfidic cross-links. Slowing down of glassy dynamics was found for all sulfur-cured elastomers with respect to the uncured ones because of an increase in the frictional coefficient. Correspondingly, higher glass transition temperatures were estimated for vulcanized elastomers, which linearly increased with the cross-link density. On the other hand, polymer fragility seems to be substantially unaffected by vulcanization.

The effect of cross-linking on collective chain dynamics was investigated by separating the contribution of polymer dynamics to ^{1}H longitudinal relaxation from that of glassy dynamics for uncured and, for the first time in this work, for vulcanized elastomers. In all cases, the fractional contribution of polymer dynamics was found to be very small (0.05−0.14), and no significant dependence on the cross-link density was observed because of an intrinsic insensitivity of the procedure. A larger contribution of polymer dynamics was found for elastomers of the BR and SBR series with respect to those of the IR one, ascribable to the different structures of the monomeric units, which in BR and SBR present a spin pair along the double bonds, resulting in an increased dynamic order parameter. In the investigated frequency range, polymer dynamics in regimes I and II of tube reptation theory was observed for all uncross-linked elastomers, regime II being better observed for BR because of its lower T_g. On the contrary, only regime I was detected for most cross-linked elastomers, indicating that permanent cross-links impose constraints on dynamics occurring on a larger scale than free Rouse modes, while they do not significantly affect the spectrum of Rouse dynamics. The deviation from regime I observed at the lowest frequencies and highest temperatures for the BR sample with the lowest cross-link density suggests that for lightly cross-linked rubbers, larger space and time scale dynamics could occur far above T_g. In this respect, because FC NMR measurements at higher temperatures are not possible because of sample stability, it could be useful to perform experiments at much lower frequencies, exploiting home-built relaxometers with compensation for earth and stray magnetic fields.[31]

ASSOCIATED CONTENT

Supporting Information

The Supporting Information is available free of charge at https://pubs.acs.org/doi/10.1021/acs.macromol.0c01439.

^{1}H NMR susceptibility curves; ^{1}H NMRD curves, $\chi''(\omega\tau_s)$ master curves, τ_s versus $1000/T$, and $\mathrm{Log}\tau_s$ versus $T/T_g - 1$ curves of IR-based vulcanized samples with different contents of polysulfidic bridges; R_1/τ_s versus $\omega\tau_s$ master curves; cross-link density versus sulfur content curves; and spectral decompositions of $\chi''(\omega\tau_s)$ (PDF)

AUTHOR INFORMATION

Corresponding Authors

Marco Geppi − Dipartimento di Chimica e Chimica Industriale, Università di Pisa, 56124 Pisa, Italy; Istituto di Chimica dei Composti OrganoMetallici, Consiglio Nazionale Delle Ricerche, 56124 Pisa, Italy; orcid.org/0000-0002-2422-8400; Phone: +39 0502219289; Email: marco.geppi@unipi.it

Lucia Calucci − Istituto di Chimica dei Composti OrganoMetallici, Consiglio Nazionale Delle Ricerche, 56124 Pisa, Italy; orcid.org/0000-0002-3080-8807; Phone: +39 0503152517; Email: lucia.calucci@pi.iccom.cnr.it

Authors

Francesca Martini − Dipartimento di Chimica e Chimica Industriale, Università di Pisa, 56124 Pisa, Italy; Istituto di Chimica dei Composti OrganoMetallici, Consiglio Nazionale Delle Ricerche, 56124 Pisa, Italy

Elisa Carignani − Dipartimento di Chimica e Chimica Industriale, Università di Pisa, 56124 Pisa, Italy; Istituto di Chimica dei Composti OrganoMetallici, Consiglio Nazionale Delle Ricerche, 56124 Pisa, Italy; orcid.org/0000-0001-5848-9660

Francesca Nardelli − Dipartimento di Chimica e Chimica Industriale, Università di Pisa, 56124 Pisa, Italy; Istituto di Chimica dei Composti OrganoMetallici, Consiglio Nazionale Delle Ricerche, 56124 Pisa, Italy

Elena Rossi − Dipartimento di Chimica e Chimica Industriale, Università di Pisa, 56124 Pisa, Italy

Silvia Borsacchi − Istituto di Chimica dei Composti OrganoMetallici, Consiglio Nazionale Delle Ricerche, 56124 Pisa, Italy; orcid.org/0000-0003-3696-0719

Mattia Cettolin − Pirelli Tyre SpA, 20126 Milano, Italy

Antonio Susanna − Pirelli Tyre SpA, 20126 Milano, Italy

Complete contact information is available at:
https://pubs.acs.org/10.1021/acs.macromol.0c01439

Author Contributions

The manuscript was written through contributions of all authors. All authors have given approval to the final version of the manuscript.

Notes

The authors declare no competing financial interest.

■ REFERENCES

(1) Rouse, P. E. A Theory of the Linear Viscoelastic Properties of Dilute Solutions of Coiling Polymers. *J. Chem. Phys.* **1953**, *21*, 1272−1280.

(2) De Gennes, P. G. Reptation of a Polymer Chain in the Presence of Fixed Obstacles. *J. Chem. Phys.* **1971**, *55*, 572−579.

(3) Doi, M.; Edwards, S. F. *The Theory of Polymer Dynamics*; Science Publication: Oxford, London, 1986.

(4) Fatkullin, N.; Kimmich, R.; Weber, H. W. Spin-lattice Relaxation of Polymers: The Memory-Function Formalism. *Phys. Rev. E: Stat. Phys., Plasmas, Fluids, Relat. Interdiscip. Top.* **1993**, *47*, 4600−4603.

(5) Fatkullin, N.; Kimmich, R. Nuclear spin-lattice relaxation dispersion and segment diffusion in entangled polymers. Renormalized Rouse formalism. *J. Chem. Phys.* **1994**, *101*, 822−832.

(6) Kroutieva, M.; Fatkullin, N.; Kimmich, R. Polymer Chain Dynamics Predicted by n-Renormalized Rouse Models: Numerical Studies. *Macromol. Symp.* **2004**, *217*, 267−272.

(7) Krutyeva, M.; Fatkullin, N.; Kimmich, R. Numerical Study of Dynamical Properties of Entangled Polymer Melts in Terms of Renormalized Rouse Models. *Polym. Sci., Ser. A* **2005**, *47*, 1022−1031.

(8) Schweizer, K. S. Microscopic theory of the dynamics of polymeric liquids: General formulation of a mode-mode-coupling approach. *J. Chem. Phys.* **1989**, *91*, 5802−5821.

(9) Schweizer, K. S. Mode-coupling theory of the dynamics of polymer liquids: Qualitative predictions for flexible chain and ring melts. *J. Chem. Phys.* **1989**, *91*, 5822−5839.

(10) Weber, H. W.; Kimmich, R. Anomalous segment diffusion in polymers and NMR relaxation spectroscopy. *Macromolecules* **1993**, *26*, 2597−2606.

(11) Lang, M.; Sommer, J.-U. Analysis of Entanglement Length and Segmental Order Parameter in Polymer Networks. *Phys. Rev. Lett.* **2010**, *104*, 177801.

(12) Lang, M. Monomer Fluctuations and the Distribution of Residual Bond Orientations in Polymer Networks. *Macromolecules* **2013**, *46*, 9782−9797.

(13) Hagen, R.; Salmén, L.; Stenberg, B. Effects of the Type of Crosslink on Viscoelastic Properties of Natural Rubber. *Polym. Sci., Ser. B* **1996**, *34*, 1997−2006.

(14) Schroeder, M. J.; Roland, C. M. Segmental Relaxation in End-Linked Poly(dimethylsiloxane) Networks. *Macromolecules* **2002**, *35*, 2676−2681.

(15) Robertson, C. G.; Wang, X. Nanoscale Cooperative Length of Local Segmental Motion in Polybutadiene. *Macromolecules* **2004**, *37*, 4266−4270.

(16) Shen, J.; Lin, X.; Liu, J.; Li, X. Effects of Cross-Link Density and Distribution on Static and Dynamic Properties of Chemically Cross-Linked Polymers. *Macromolecules* **2019**, *52*, 121−134.

(17) Kramarenko, V. Y.; Ezquerra, T. A.; Sics, I.; Baltá-Calleja, F. J.; Privalko, V. P. Influence of Cross-Linking on the Segmental Dynamics in Model Polymer Networks. *J. Chem. Phys.* **2000**, *113*, 447−452.

(18) Dueñas, J. M. M.; Mateo, J. M.; Ribelles, J. L. G. Influence of the Cross-Linking Density on the Main Dielectric Relaxation of Poly(methyl acrylate) Networks. *Polym. Eng. Sci.* **2005**, *45*, 1336−1342.

(19) Kalakkunnath, S.; Kalika, D. S.; Lin, H.; Freeman, B. D. Segmental Relaxation Characteristics of Cross-Linked Poly(ethylene oxide) Copolymer Networks. *Macromolecules* **2005**, *38*, 9679−9687.

(20) Hernández, M.; Valentín, J. L.; López-Manchado, M. A.; Ezquerra, T. A. Influence of the vulcanization system on the dynamics and structure of natural rubber: Comparative study by means of broadband dielectric spectroscopy and solid-state NMR spectroscopy. *Eur. Polym. J.* **2015**, *68*, 90−103.

(21) Anoardo, E.; Galli, G.; Ferrante, G. Fast-Field-Cycling NMR: Applications and Instrumentation. *Appl. Magn. Reson.* **2001**, *20*, 365−404.

(22) Kimmich, R.; Anoardo, E. Field-Cycling NMR Relaxometry. *Prog. Nucl. Magn. Reson. Spectrosc.* **2004**, *44*, 257−320.

(23) Kimmich, R. *Field-Cycling NMR Relaxometry: Instrumentation, Model Theories and Applications*; Royal Society of Chemistry: Cambridge, 2019.

(24) Kimmich, R.; Fatkullin, N. Polymer Chain Dynamics and NMR. *Advances in Polymer Science*; Springer, 2004; Vol. *170*, pp 1−113.

(25) Kariyo, S.; Gainaru, C.; Schick, H.; Brodin, A.; Novikov, V. N.; Rössler, E. A. From a Simple Liquid to a Polymer Melt: NMR Relaxometry Study of Polybutadiene. *Phys. Rev. Lett.* **2006**, *97*, 207803. Herrmann, A.; Gainaru, C.; Schick, H.; Brodin, A.; Novikov, V. N.; Rössler, E. A. Erratum: From a Simple Liquid to a Polymer Melt: NMR Relaxometry Study of Polybutadiene [Phys. Rev. Lett.97, 207803 (2006)]. *Phys. Rev. Lett.* **2008**, *100*, 109901.

(26) Kariyo, S.; Brodin, A.; Gainaru, C.; Herrmann, A.; Schick, H.; Novikov, V. N.; Rössler, E. A. From Simple Liquid to Polymer Melt. Glassy and Polymer Dynamics Studied by Fast Field Cycling NMR Relaxometry: Low and High Molecular Weight Limit. *Macromolecules* **2008**, *41*, 5313−5321.

(27) Kariyo, S.; Brodin, A.; Gainaru, C.; Herrmann, A.; Hintermeyer, J.; Schick, H.; Novikov, V. N.; Rössler, E. A. From Simple Liquid to Polymer Melt. Glassy and Polymer Dynamics Studied by Fast Field Cycling NMR Relaxometry: Rouse Regime. *Macromolecules* **2008**, *41*, 5322−5332.

(28) Herrmann, A.; Novikov, V. N.; Rössler, E. A. Dipolar and Bond Vector Correlation Function of Linear Polymers Revealed by Field Cycling 1H NMR: Crossover from Rouse to Entanglement Regime. *Macromolecules* **2009**, *42*, 2063−2068.

(29) Herrmann, A.; Kariyo, S.; Abou Elfadl, A.; Meier, R.; Gmeiner, J.; Novikov, V. N.; Rössler, E. A. Universal Polymer Dynamics Revealed by Field Cycling 1H NMR. *Macromolecules* **2009**, *42*, 5236−5243.

(30) Hofmann, M.; Herrmann, A.; Abou Elfadl, A.; Kruk, D.; Wohlfahrt, M.; Rössler, E. A. Glassy, Rouse, and Entanglement Dynamics As Revealed by Field Cycling 1H NMR Relaxometry. *Macromolecules* **2012**, *45*, 2390−2401.

(31) Herrmann, A.; Kresse, B.; Gmeiner, J.; Privalov, A. F.; Kruk, D.; Fujara, F.; Rössler, E. A. Protracted Crossover to Reptation Dynamics: A Field Cycling 1H NMR Study Including Extremely Low Frequencies. *Macromolecules* **2012**, *45*, 1408−1416.

(32) Hofmann, M.; Kresse, B.; Privalov, A. F.; Willner, L.; Fatkullin, N.; Fujara, F.; Rössler, E. A. Field-Cycling NMR Relaxometry Probing the Microscopic Dynamics in Polymer Melts. *Macromolecules* **2014**, *47*, 7917−7929.

(33) Fatkullin, N.; Stapf, S.; Hofmann, M.; Meier, R.; Rössler, E. A. Proton spin dynamics in polymer melts: New perspectives for experimental investigations of polymer dynamics. *J. Non-Cryst. Solids* **2015**, *407*, 309−317.

(34) Kimmich, R.; Fatkullin, N. Self-diffusion studies by intra- and inter-molecular spin-lattice relaxometry using field-cycling: Liquids, plastic crystals, porous media, and polymer segments. *Prog. Nucl. Magn. Reson. Spectrosc.* **2017**, *101*, 18−50.

(35) Rössler, E. A.; Hofmann, M.; Fatkullin, N. Application of Field-Cycling ¹H NMR Relaxometry to the Study of Translational and Rotational Dynamics in Liquids and Polymers. In *Field-Cycling NMR Relaxometry: Instrumentation, Model Theories and Applications*; Kimmich, R., Ed.; The Royal Society of Chemistry: Cambridge, 2019; Chapter 8, pp 181−206.

(36) Stapf, S.; Lozovoi, A. Field-Cycling Relaxometry of Polymers. In *Field-Cycling NMR Relaxometry: Instrumentation, Model Theories and Applications*; Kimmich, R., Ed.; The Royal Society of Chemistry: Cambridge 2019; Chapter 13, pp 322−357.

(37) Ferry, J. D. *Viscoelasticity Properties of Polymers*; John Wiley & Sons Ltd: New York, 1980.

(38) Ding, Y.; Sokolov, A. P. Breakdown of Time−Temperature Superposition Principle and Universality of Chain Dynamics in Polymers. *Macromolecules* **2006**, *39*, 3322−3326.

(39) Kimmich, R.; Gille, K.; Fatkullin, N.; Seitter, R.; Hafner, S.; Müller, M. Field-Cycling Nuclear Magnetic Resonance Relaxometry

of Thermoreversible Polybutadiene Networks. *J. Chem. Phys.* **1997**, *107*, 5973−5978.

(40) Kariyo, S.; Stapf, S. Influence of Cross-Link Density and Deformation on the NMR Relaxation Dispersion of Natural Rubber. *Macromolecules* **2002**, *35*, 9253−9255.

(41) Kariyo, S.; Stapf, S. NMR Relaxation Dispersion of Vulcanized Natural Rubber. *Solid-State NMR Spectrosc.* **2004**, *25*, 64−71.

(42) Kariyo, S.; Stapf, S. Restricted Molecular Dynamics of Polymer Chains by Means of NMR Field Cycling Relaxometry. *Macromol. Chem. Phys.* **2005**, *206*, 1300−1310.

(43) Stapf, S.; Kariyo, S.; Blümich, B. Correlating Molecular and Macroscopic Properties of Elastomers by NMR Relaxometry and Multi-pulse NMR Techniques. *Modern Magnetic Resonance*; Webb, G. A., Ed.; Springer, 2006; pp1435−1441.

(44) Bloembergen, N.; Purcell, E. M.; Pound, R. V. Relaxation Effects in Nuclear Magnetic Resonance Absorption. *Phys. Rev.* **1948**, *73*, 679−712.

(45) Böttcher, C. J. F.; Bordewijk, P. *Theory of Electric Polarization*; Elsevier Scientific: Amsterdam, 1978; Vol. *II*.

(46) Schönhals, A.; Kremer, F. *Broadband Dielectric Spectroscopy*; Kremer, F., Schönhals, A., Eds.; Springer-Verlag: Berlin, 2003.

(47) Blochowicz, T.; Gainaru, C.; Medick, P.; Tschirwitz, C.; Rössler, E. A. The Dynamic Susceptibility in Glass Forming Molecular Liquids: The Search for Universal Relaxation Patterns II. *J. Chem. Phys.* **2006**, *124*, 134503.

(48) Saville, B.; Watson, A. A. Structural Characterization of Sulfur-Vulcanized Rubber Networks. *Rubber Chem. Technol.* **1967**, *40*, 100−148.

(49) Sebastião, P. J. Fitteia. Fitting Environment Interfaces for All. http://fitteia.org (date last accessed: May 20, 2020).

(50) Sebastião, P. J. The Art of Model Fitting to Experimental Results. *Eur. J. Phys.* **2014**, *35*, 015017.

(51) *Mathematica*, Version 10; Wolfram Research, Inc.: Champaign, IL, 2010.

(52) Kariyo, S.; Stapf, S.; Blümich, B. Site Specific Proton and Deuteron NMR Relaxation Dispersion in Selectively Deuterated Polyisoprene Melts. *Macromol. Chem. Phys.* **2005**, *206*, 1292−1299.

(53) Kimmich, R.; Fatkullin, N.; Seitter, R.-O.; Gille, K. Chain Dynamics in Entangled Polymers: Power Laws of the Proton and Deuteron Spin-Lattice Relaxation Dispersions. *J. Chem. Phys.* **1998**, *108*, 2173−2177.

(54) Jenczyk, J.; Dobies, M.; Makrocka-Rydzyk, M.; Wypych, A.; Jurga, S. The segmental and global dynamics in lamellar microphase-separated poly(styrene-b-isoprene) diblock copolymer studied by 1H NMR and dielectric spectroscopy. *Eur. Polym. J.* **2013**, *49*, 3986−3997.

(55) Furtado, F.; Damron, J.; Trutschel, M.-L.; Franz, C.; Schröter, K.; Ball, R. C.; Saalwächter, K.; Panja, D. NMR Observations of Entangled Polymer Dynamics: Focus on Tagged Chain Rotational Dynamics and Confirmation from a Simulation Model. *Macromolecules* **2014**, *47*, 256−268.

(56) Trutschel, M.-L.; Mordvinkin, A.; Furtado, F.; Willner, L.; Saalwächter, K. Time-Domain NMR Observation of Entangled Polymer Dynamics: Focus on All Tube-Model Regimes, Chain Center, and Matrix Effects. *Macromolecules* **2018**, *51*, 4108−4117.

(57) Wang, Z.; Likhtman, A. E.; Larson, R. G. Segmental Dynamics in Entangled Linear Polymer Melts. *Macromolecules* **2012**, *45*, 3557−3570.

(58) Panja, D.; Barkema, G. T.; Ball, R. C. Complex Interactions with the Surroundings Dictate a Tagged Chain's Dynamics in Unentangled Polymer Melts. *Macromolecules* **2015**, *48*, 1442−1453.

(59) Fetters, L. J.; Lohse, D. J.; Richter, D.; Witten, T. A.; Zirkel, A. Connection Between Polymer Molecular Weight, Density, Chain Dimensions, and Melt Viscoelastic Properties. *Macromolecules* **1994**, *27*, 4639−4647.

(60) Ueberreiter, K.; Kanig, G. Second-Order Transitions and Mesh Distribution Functions of Cross-Linked Polystyrenes. *J. Chem. Phys.* **1950**, *18*, 399−406.

(61) Fox, T. G.; Loshaek, S. Influence of Molecular Weight and Degree of Crosslinking on the Specific Volume and Glass Temperature of Polymers. *J. Polym. Sci.* **1955**, *15*, 371−390.

(62) Nielsen, L. E. Cross-Linking-Effect on Physical Properties of Polymers. *J. Macromol. Sci., Polym. Rev.* **1969**, *3*, 69−103.

(63) Chang, S.-S. Effect of Curing History on Ultimate Glass Transition Temperature and Network Structure of Crosslinking Polymers. *Polymer* **1992**, *33*, 4768−4778.

(64) Bandzierz, K.; Reuvekamp, L.; Dryzek, J.; Dierkes, W.; Blume, A.; Bielinski, D. Influence of Network Structure on Glass Transition Temperature of Elastomers. *Materials* **2016**, *9*, 607.

(65) Bandzierz, K. S.; Reuvekamp, L. A. E. M.; Dryzek, J.; Dierkes, W. K.; Blume, A.; Bieliński, D. M. Effect of Polymer Chain Modifications on Elastomer Properties. *Rubber Chem. Technol.* **2019**, *92*, 513−530.

(66) Saalwächter, K.; Heuer, A. Chain Dynamics in Elastomers as Investigated by Proton Multiple-Quantum NMR. *Macromolecules* **2006**, *39*, 3291−3303.

(67) Saalwächter, K.; Herrero, B.; López-Manchado, M. A. Chain Order and Cross-Link Density of Elastomers as Investigated by Proton Multiple-Quantum NMR. *Macromolecules* **2005**, *38*, 9650−9660.

(68) Vaca Chávez, F.; Saalwächter, K. Time-Domain NMR Observation of Entangled Polymer Dynamics: Universal Behavior of flexible Homopolymers and Applicability of the Tube Model. *Macromolecules* **2011**, *44*, 1549−1559.